Sensitivity Analysis and Robust Optimization of an Integrated Pneumatic End-Position Cushioning

Fedor Nazarov, Jürgen Weber

Technische Universität Dresden, Institute of Mechatronic Engineering, Chair of Fluid-Mechatronic Systems,
Helmholzstrasse 7a, D-01069 Dresden, Germany
E-Mail: fedor.nazarov@tu-dresden.de

In this paper an analysis and a robust optimization of a validated simulation model representing an integrated pneumatic end cushioning is proposed. The aim is to optimize the geometrical parameters of the standard end cushioning unit, such as cushioning sleeve diameter, length, and dead volume, in order to improve the damping performance. By means of the robust optimization both impact force and piston travel time are reduced, whereas the robustness against fluctuating operational conditions, such as supply pressure or inertial load, is increased. It is also shown that the pneumatic frequency ratio (PFR) is applicable for the damping capability assessment of a well-sized cylinder. It can be also used as a dimensionless criterion for prediction of the cushioning setting needed for a particular application.

Keywords: Pneumatics, end cushioning, pneumatic cylinder, energy efficiency, robust optimization.
Target audience: Pneumatics, Automation and Handling Systems, Design Process.

1 Introduction

Pneumatically driven systems are widely applied in numerous branches. The robotics, medicine, food industry and automotive sector highlight only some of them. Pneumatics deserves a reputation of a reliable, hygienic, and user-friendly technology, although it is not free from some drawbacks. Its major weakness is a relatively high energy consumption compared to electromechanical systems.

United in a common purpose to increase the energy efficiency of pneumatic systems while keeping low the acquisition costs, many energy saving measures were invented, elaborated, and tested within the last decades. One of the simplest and most effective approaches is a correct cylinder sizing. However, in some applications the cylinders are still deliberately oversized. The oversizing is especially distinctive for motion tasks, where external force and friction are significantly lower than inertial force of the moved mass.

1.1 Related problem and subject

When talking about the motion tasks, pneumatic drives are usually operated at a minimum tact time to achieve the maximum machine productivity. This requests both high acceleration and high deceleration capability of a pneumatic drive. Whilst a rapid pressure build-up in the cylinder chamber easily ensures the fast acceleration, the decrease of kinetic energy by the end of the stroke is often very challenging. The only one standard measure designed for this purpose is a pneumatic end-position cushioning, which is integrated in most cylinders larger than Ø10…16 mm. However, the damping capability of this type of cushioning is limited and sets certain boundaries on maximum travel speed and handled mass. As the damping capability increases with the cylinder's diameter, a deficient cushioning behaviour is one of the main reasons for the point-to-point-operated cylinders being oversized. As a result of insufficient damping capability, larger cylinders are often preferred in the applications, even if a smaller cylinder would be enough to move the mass within the given time. This results in a higher amount of consumed compressed air. In the literature large-scaling is assessed to be typical for nearly 80 % of all applications and raises the energy consumption up to 40 % [1].

Besides, the damping performance of the integrated end cushioning is very sensitive against any changes in travel speed, cushioning throttle setting, supply pressure, load mass, and some further factors. Another deficiency of the classical end cushioning is an absence of any method available for an exact calculation of the desired cushioning throttle setting. Instead, the cushioning throttle is adjusted manually by a try-and-error nature, is very tedious and time demanding.

Among the standard pneumatic cushioning there are some other technologies designed to solve or at least to mitigate the above written problems. Almost all of them can be classified as hydraulic shock absorbers [2], elastomer mechanical cushioning [3], electronically controlled external pneumatic end cushioning [4][5], devices for an assisted cushioning throttle setting [6], or sophisticated modifications of the standard pneumatic end cushioning design [7]. However, these options are either costly, require additional installation space, or provide performance increase only in some selective operational points. For this reason, the simple, compact, and non-expensive integrated pneumatic end cushioning still remains the mostly applied damping device and therefore is the subject of the current study.

Previous investigations, also dedicated to this subject, pursued an aim to elaborate a valid mathematical model of the pneumatic cushion and to understand the interrelations between the damping behaviour and the operational conditions of the cylinder [8]–[10]. In [11] an empirical-analytical method for design of the cushioning devices is proposed as well. However, there is no study dealing with the design optimization of the integrated pneumatic cushion known to the authors.

Summing up, the current method of decelerating the load of a pneumatic cylinder is coupled with time-demanding commissioning and maintenance, is not robust at fluctuating operating conditions, and often leads to an oversizing in case of high-inertia and high-speed motion tasks. The alternative technologies mitigate some of these drawbacks though but are not very widely used due to additional acquisition costs or installation space.

1.2 The aim of the study

Hence, this paper focuses on a systematic improvement of the damping performance of the classical integrated pneumatic end cushioning. The goal is to determine the design parameters with a major influence on the ability of the end cushioning to absorb the kinetic energy of the moving mass and to perform the robust optimization of these parameters. This knowledge can either enable an implementation of the cushioning device with a traditional design, but geometrical parameters tuned for a better performance, or can help to derive a novel design from the sensitivity analysis and robust optimization results. For the sake of simplicity, the formulation of the global goal as “improvement of the damping performance” can be decomposed into the following qualities that are aimed to increase:

1. The damping capability: to enable a safe deceleration at high travel speed, high inertial load or at low pressure in the deflated cylinder chamber. The latter can increase the applicability of the energy efficient meter-in throttling speed control, which is currently less favored then the less-efficient meter-out throttling int. al. because of a poor damping performance due to a low initial value of the cushion pressure.
2. The robustness against the changes in environmental and operational conditions: to guarantee a safe deceleration at fluctuating travel speed, supply pressure, inertial load, and environmental temperature without a need to manipulate the cushion setting each time one of these parameters is changed.
3. The user-friendliness: to ease the process of the cushioning throttle setting and to provide the method for calculation and prediction of the throttle setting needed for a particular application.

Since all these qualities are interdependent, improving one of them may indirectly result in the improvement of another one. The criteria of “safe deceleration“ are disclosed in the paragraph 2.2.

The object of the research is the mathematical model of the pneumatic cylinder with an integrated end cushioning that was previously presented and comprehensively validated by authors in [12][13].

2 Modell Analysis

In this section the scope of the research is stated in terms of the studied system, criteria applied for the evaluation of the damping quality, and estimation of the reasonable operating range of the drive. This helps to generalize the knowledge obtained for one specific cylinder and to make it transferable for other applications.

2.1 Studied system

A typical design of the pneumatic cylinder with an end cushioning is shown in the **Figure 1**. When considering the retraction stroke, left chamber is pressurized with air at pressure nearly equal to the supply pressure $p_A \approx p_0$. A piston, coupled mechanically with an inertial load m, moves to the right base end 2 displacing the air from the opposite chamber at pressure p_B. Here the commonly used meter-out throttle speed control is considered. Both mean travel speed and travel time t_s depend on the conductance of the throttle 5. As soon as the chamfer of the cushion sleeve 1 overlaps the cushion sealing of the base end 2, the right cylinder chamber becomes divided into two volumes: the cushioning volume 6 and the dead volume 3 of the cylinder base end. The cushioning volume is connected with the outflow channel only via the bypassed cushioning throttle with a high resistance that causes an increase of pressure p_{EC} in the cushioning volume. The increased pressure force, applied on the right piston surface, counteracts to the moving force, caused by inertia and p_A, and decelerates the cylinder.

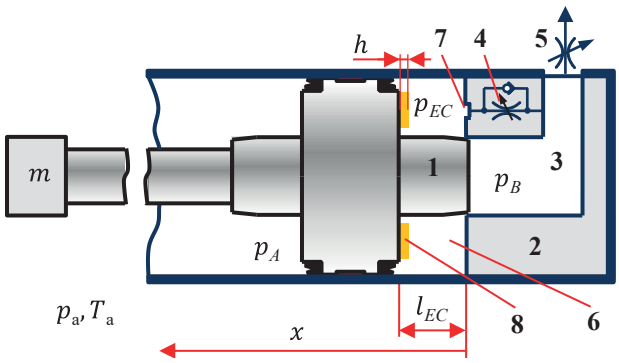


Figure 1: Simplified scheme of a pneumatic cushioning: 1 – end cushioning plug (sleeve), 2 – base end, 3 – outflow channel with dead volume V_d, 4 – end cushioning throttle (bypass channel), 5 – meter-out throttle, 6 – cushioning volume, 7 - stroke-independent cushioning dead volume V_{EC}, 8 – elastomer shock absorber.

The present research is based on the mathematical model of the pneumatic cylinder with diameter of Ø32 mm and stroke of 100 mm described and experimentally validated in [12][13]. For the sake of compactness the mathematical background of this model is skipped here. In this study it is treated as a function $\mathbf{y} = f(\mathbf{x}, \mathbf{u})$ of evaluation criteria $\mathbf{y}$ depending on the design parameters $\mathbf{x}$ that are expected to have an impact on these criteria, and the noise parameters $\mathbf{u}$ that represent uncertain fluctuating operational parameters. The focus lies on the robust optimization, i. e. on search for geometrical parameters of the cushioning unit allowing the minimal values of the evaluation criteria y_i in the presence of fluctuating noise parameters subject to the technically reasonable boundaries of the design parameters $g(\mathbf{x})$ and noise parameters $h(\mathbf{u})$:

$$\min_{\mathbf{x}\in\mathbb{R}^n,\ \mathbf{u}\in\mathbb{R}^k} \{f_i(\mathbf{x},\mathbf{u}) : \quad g(\mathbf{x}) \le 0, \qquad h(\mathbf{u}) \le 0, \qquad i = 1, \dots m\}. \tag{1}$$

2.2 Evaluation of the cushioning quality

Generally, the behaviour of the piston in the end cushioning may be classified as optimal, underdamped, or overdamped. It depends on the supply pressure p_0, travel speed $\dot{x}$ set by the meter-out throttle conductance C_{MO} (or a number of throttle knob revolutions z_{MO}, i. e. the throttle opening), conductance of the end-cushioning throttle C_{EC} (or z_{EC}), and the moving mass m. **Figure 2** illustrates these three typical scenarios for a well-sized pneumatic drive intended to have a travel time of $t_s = 0.3$ s and tolerated settling error, i. e. a threshold under which the piston movement is treated as finished, of $x_{thr} = 0.5$ mm. The required t_s is usually prescribed by an application and should

be considered for efficient cylinder sizing, as it will be discussed in the paragraph 2.3. The threshold value x_{thr} can be set to zero, if an exact end-positioning of the load is requested. This value can depend on the location of an end switch, mounted on the cylinder body, as well as on its sensing region that may amount up to few millimeters. The value x_{thr} = 0.5 mm will be consistently used throughout the entire paper.

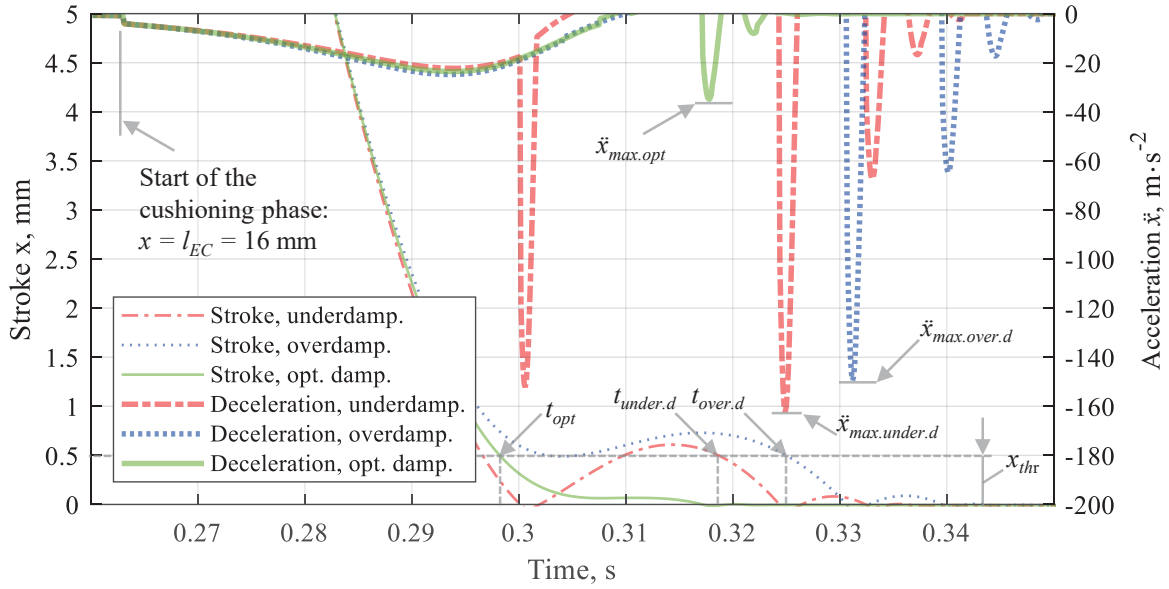


Figure 2: Cylinder stroke x and deceleration ẍ plotted for three scenarios of the cushioning phase for a studied Ø32-100-cylinder operated at p_0 = 7 bar_{abs} with inertial load m = 18.1 kg and desired travel time t_s = 0.3 s.

In this example the end cushioning throttle opening z_{EC} is varied around some nearly optimal value to reach the underdamping (wide opening z_{EC}, i. e. low throttle resistance C_{EC}) and overdamping (low z_{EC}, high C_{EC}) for the illustrative purpose. In both cases, underdamping and overdamping, the real travel time t_s, increases due to a piston retraction from the cylinder base end or from the air cushion respectively. This results in a longer travel time $t_s > 0.3$ s. When varying z_{EC} in a wider range, or varying additionally some operational parameters, travel time may increase dramatically, up to many times. This behaviour causes deteriorations in an automated processes and degrades the machine productiveness, e. g. when the end switch is crossed for several times within only one stroke and this is faulty treated by the PLC programme, or when the other drives in the automation chain have to wait for the positioning of the considered cylinder below the x_{thr}.

The next point that catches an attention is a rapid increase in the negative acceleration (deceleration) with deviation from the optimal z_{EC} setting. This may be not always the case for a highly oversized and overdamped cylinder that reaches a stationary speed in the cushioning region and travels very slowly until the end stop. However, the peak deceleration increases always when opening the cushioning throttle to wide or overloading the cylinder (i. e. operating it with too high mass or speed). The underdamping is always crucial because it results in a high impact force F_{impact}, which causes vibrations, noise, and mechanical stress. It is difficult to set some general level of an acceptable acceleration amplitude, because it depends on the manufacturer-specific stiffness c and thickness h of the elastomer layer, applied on the frontal face of the piston or cylinder end to absorb the residual kinetic energy:

$$F_{impact} = m \cdot \max(\ddot{x}) \sim c \cdot (h - x)\,. \tag{2}$$

In the given study the value of maximum tolerable impact force is assessed with 1 kN, which is about the theoretical static cylinder force at the maximum operating pressure of 12 bar_{rel}. Under this assumption the cylinder would never be subject to the stress higher than two times maximum static force. This also matches with the forces specified for the rod attachments, e. g. swivel rod ends for the corresponding cylinder size.

Although the value of the maximum deceleration is coupled with F_{impact} via the mass m, it can be reasonable to set the deceleration as a separate criterion of the damping quality, because an oversized drive may exceed the tolerable limit $\ddot{x}_{max}$ while not exceeding the limit of F_{impact}. For the studied system $\ddot{x}_{max}$ is considered to be $\ddot{x}_{max}$ = 50 m·s^{-2}

basing on the specifications of the maximum acceleration for some supplementary components, such as mechanical guide axes. Since the studied system doesn't refer to any specific application, both these values, F_{impact} and $\ddot{x}_{max}$, are used here only as indicative quantitative criteria for the evaluation of the damping process.

On this place can be mentioned that the example in Figure 2 also illustrates the high sensitivity of the damping behaviour against the throttle opening z_{EC}. The difference between the optimal and each of the non-optimal settings corresponds to about ±32° of a throttle knob revolution (9 % of a full revolution). As the cushioning throttle in the considered cylinder has a setting range of four full revolutions, this value corresponds to only 2.25 % of the full range, what implies the search for the optimal setting to be difficult for an end-user.

Summing up, the three criteria: travel time t_s, impact force F_{impact} and peak deceleration $\ddot{x}_{max}$ are expected to be enough to characterize the quality of a damping process. Other criteria, such as maximum amount of absorbed kinetic energy, travel speed before meeting the end stop, or cushioning phase duration are also suitable. Since they correlate with the chosen criteria and are more difficult to generalize, they are not considered here.

2.3 Operating range of the considered drive

To reduce the space of the parameters that are varied during the investigation and to preserve the representativeness of the results for a multitude of non-considered cases, operational points must be chosen properly for the study. As it was already mentioned in the introduction, the cushioning problem is especially crucial for the cylinders that operate on the limit of their cushioning capability, i. e. with maximum combination of inertial load and speed at the given pressure. Besides, the cushioning capability depends on the piston areas of the cylinder. In this context the Pneumatic Frequency Ratio (PFR) proposed by Doll et al. in [14], is perfectly suitable as a sizing factor that helps to generalize different applications with regards to the cylinder load and cushioning capability. The PFR Ω is defined as a ratio of the cylinder eigenfrequency ω_0 and operating frequency ω_S [14]:

$$\Omega = \frac{\omega_0}{\omega_s}. \tag{3}$$

The operating frequency can be estimated from the travel time (transition time) of the piston as $\omega_s = 2\pi/t_s$, specified for the motion task. The eigenfrequency of the pneumatic cylinder with inertial load corresponds to those of the mechanical spring-mass system, with a stiffness factor c depending on the supply pressure p_0 and the pressurized volumes V_A and V_B of both cylinder chambers including the dead and the hose volumes:

$$\omega_0 = \sqrt{\frac{c}{m}} = \sqrt{\frac{c_A + c_B}{m}} = \sqrt{\frac{\frac{A_A^2 \cdot \nu \cdot p_0}{V_A} + \frac{A_B^2 \cdot \nu \cdot p_0}{V_B}}{m}}. \tag{4}$$

The polytropic exponent ν is assumed to be $\nu = 1$ here, standing for an isothermal state change. This refers to the temperature measurements inside of the cylinder indicating an increase in 30…40 °C during the pressure build-up followed by a very fast, i. e. under 0.1 s, temperature equalization due to a high surface, heat capacity and thermal conductivity of the cylinder [13]. Hence, air temperature during the main stroke can be generally treated as nearly constant. This should be not confused with air temperature in the cushioning volume during the damping phase.

Depending on the Ω, a cylinder can be classified as an undersized ($\Omega < 1.1$), oversized ($\Omega > 1.7$) and well-dimensioned ($1.1 < \Omega < 1.7$) [14]. Low values of Ω correspond to a poor damping quality (high $\ddot{x}_{max}$, long t_s due to a piston bounce). A cylinder operating at high Ω is easy to decelerate, however it consumes more compressed air. The point of interest is some optimal value of Ω_{opt} that enables the lowest air consumption while faultlessly performing the moving task, that is task-specific criteria t_s, F_{impact}, $\ddot{x}_{max}$ are being met. To find the Ω_{opt} and analyse the damping behaviour of the cylinder, these criteria were computed for three pressure levels $p_0 \in \{4, 7, 10\}$ bar_{abs} and the range of $\Omega \in \{1.4, 1.5, 1.6, 1.8, 2\}$ for combinations of meter-out throttle openings z_{MO} and cushioning throttle openings z_{EC} that enable the desired travel time of $t_s = 0.3$ s. At $\Omega \leq 1.8$ these combinations lie in the range of $z_{EC} = 1…2$ out of maximum 4 throttle knob revolutions and $z_{MO} = 14.8…16$ out of max. 17.5 rev. However, this range migrates to larger meter-out throttle openings for the oversized cylinders ($\Omega \geq 2$). The conductance-opening

characteristics of both throttles were measured in [12]. The values of the moved masses m were calculated for each combination of Ω and p_0 from Equations (3) and (4) and are summarized in Annex A. The results, plotted in **Figure 3**, visualize the dependence of damping quality factors F_{impact}, $\ddot{x}_{max}$, and t_s, on p_0, Ω, z_{MO} and z_{EC}.

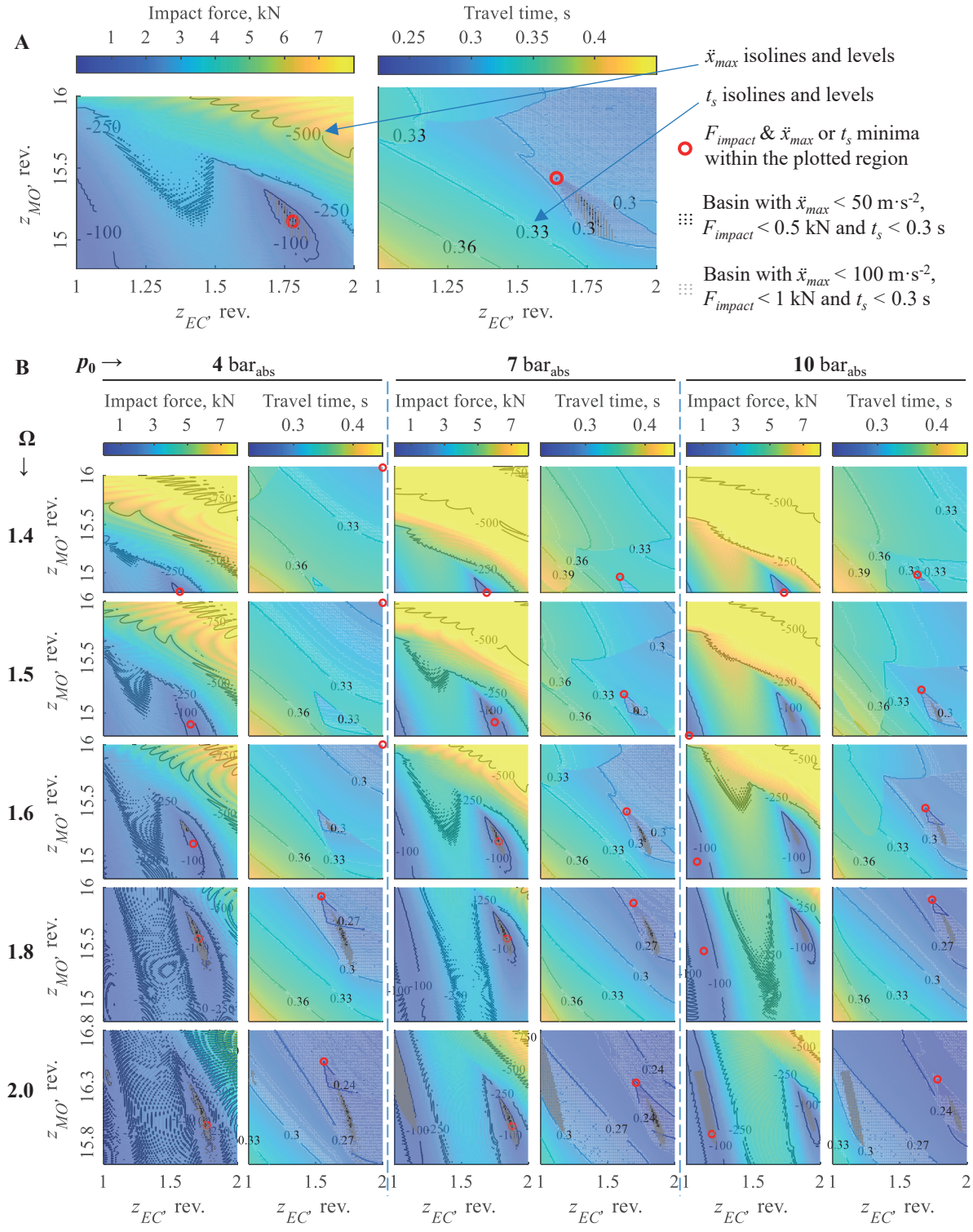


*Figure 3: **A**: Zoomed-in pair of graphs with an explanation of plotted data, **B**: Damping quality criteria: F_{impact} (left plot in the pair, colour coded), peak deceleration $\ddot{x}_{max}$ (left plot in the pair, isolines coded in m·s^{-2}), travel time t_s (right plot in the pair) at various supply pressures p_0 and PFR Ω within the ranges of cushioning and meter-out throttle openings z_{EC} and z_{MO} (in revolutions), specified to reach the desired travel time of t_s = 0.3 s.*

Each of the 15 subplot pairs represents the values of the impact force F_{impact} and travel time t_s, coded with the colour. The profile of the maximum deceleration $\ddot{x}_{max}$ is equal those of F_{impact}, as the mass m remains constant

within each separate plot. Hence, deceleration is represented only with isolines in [m·s^{-2}] layered on the F_{impact} surface. Dark-blue regions correspond to a soft landing and a fast stroke, whereas yellow regions designate a high shock and a long piston stroke respectively. A red circle marks the minimum of F_{impact} and $\ddot{x}_{max}$ or t_s contained in each plotted dataset. The regions, where the requirements are met completely, i. e.: $t_s \leq 0.3$ s, $F_{impact} \leq 0.5$ kN, and $\ddot{x}_{max} \leq 50$ m·s^{-2}, are classified as a good cushioning and marked with black dots, visible when zooming in the plot. Small grey dots depict the operation points, where the time restriction is not violated, but shock is harder: $50 < \ddot{x}_{max} \leq 100$ m·s^{-2} and $0.5 < F_{impact} \leq 1$ kN. These regions are identified as partially fulfilling the requirements.

From the Figure 3 it can be obtained that at $\Omega \leq 1.4$ none of the operating points meet these requirements, concluding an under-dimensioned cylinder behaviour. Optimal operation points start to appear at $\Omega = 1.5$ at pressures $p_0 = 7$ and 10 bar$_{abs}$. Pressure of 4 bar$_{abs}$ is not enough to provide the air cushion stiffness needed for a fast and smooth deceleration at $\Omega = 1.5$, so that an optimal value of PFR can be assessed slightly above this value in the considered case. The value of $\Omega_{opt} \approx 1.5$ can also be derived from the plots for $\Omega > 1.5$. For example, travel time of $t_s < 0.24$ s can be reached with a slightly oversized cylinder operated at $\Omega = 1.8$ at $p_0 = 10$ bar$_{abs}$.

When setting this time as t_s into Equations (3) and (4), Ω appears to be $\Omega \approx 1.5$ for the same pressure and mass. Any cylinder with a lower PFR has a deficient cushioning behavior, and any cylinder with a higher PFR travels faster and hence can be used either for faster motion tasks, or operation under lower pressure or with higher mass, resulting recursively in the estimated value of $\Omega_{opt} \approx 1.5$. Using the terminology of [14], an optimal PFR corresponds to the smallest cylinder able to meet the restrictions regarding t_s, F_{impact}, $\ddot{x}_{max}$, and therefore the cylinder with the lowest air consumption. In the reality, the cylinder diameter cannot be varied continuously due to only some standard sizes are manufactured, e. g. Ø25 is easy to find but not Ø27 mm. Thus, the diameter of almost every cylinder must be rounded up to the next standard size and a cylinder becomes "natively" slightly oversized. The optimal PFR and minimum air consumption can be reached even in this case if supply pressure is reduced with a local pressure valve. However, this cannot be used everywhere for economic reasons. Some decent oversizing is reasonable to ensure the robust drive operation under fluctuating operational parameters. Hence, the real Ω_{opt} is rather a range than a sole number. This range varies naturally for different drives and applications, depending on the tube and dead volume components in V_A and V_B, resistances of the inlet/outlet lines and valve, friction force, which is not considered in the PFR-approach, levels of acceptable $\ddot{x}_{max}$ and F_{impact}, and whether extension or retraction stroke is considered.

To visualize the areas of throttle settings with acceptable damping quality more detailly, their boundaries are extracted from the subplots for $\Omega \leq 1.8$ and summarized in the **Figure 4**. The areas with partially fulfilled requirements (grey line) increase with rising p_0 and Ω, whereas areas with complete fulfillment are totally absent for $p_0 = 10$ bar$_{abs}$. This is due to the mass m rises with an increase in p_0 at a constant Ω, resulting in a higher impact force even at a moderate deceleration.

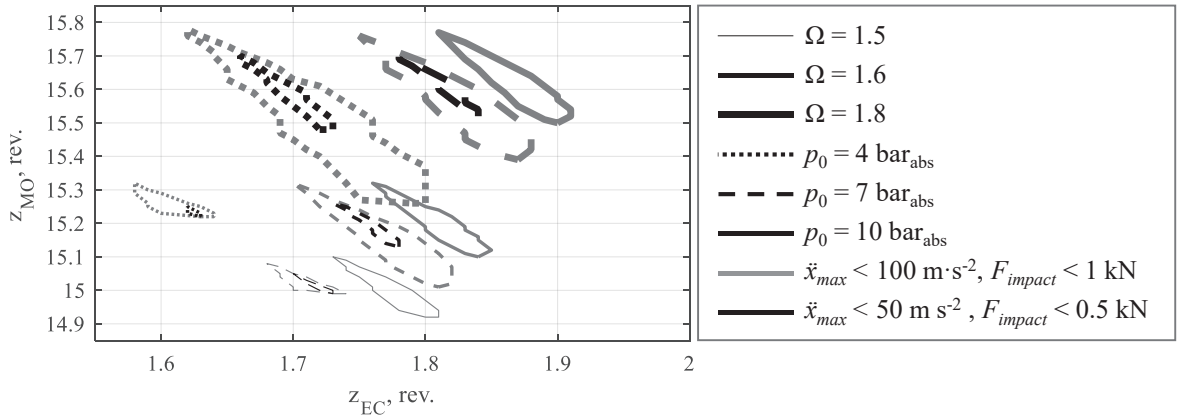


Figure 4: Boundaries of the areas of the meter-out and cushioning throttle settings corresponding to partial (grey) and complete (black) fulfilment of the requirements on the quality of the cushioning process with regards to the overall travel time t_s, impact force F_{impact}, and maximum deceleration $\ddot{x}_{max}$.

Wrapping up the discussion of the Figure 3 and Figure 4, following points must be emphasized:

- The dependencies F_{impact}, $\ddot{x}_{max} = f(z_{EC}, z_{MO})$ and $t_s = f(z_{EC}, z_{MO})$ are highly non-linear and may have multiple local minima and maxima. The form of these profiles generally and the areas of the optimal throttle settings in particular depend on the PFR Ω and supply pressure p_0.
- The higher Ω, the more combinations of z_{EC} and z_{MO} lead to a good damping and desired travel time. An oversized cylinder (in the given case with PFR above $\Omega \geq 2$) is distinguished by multiple separate areas, where these combinations exist.
- The results were also obtained for the desired travel times $t_s = 0.25$ s and $t_s = 0.5$ s. The form of the profiles for these travel times is similar to the considered here. Hence, the results of this study are also relevant for applications with other stroke lengths and tact frequencies.
- The plotted range of the cushioning throttle opening corresponds to $z_{EC} = 1\ldots2$ out of 4 rev., i. e. it represents only about a quarter of the entire range. No reasonable operation mode was found for the cushioning throttle settings $z_{EC} < 1$ and $z_{EC} > 2$. Only an oversized cylinder can be operated there, but it would always have an optimum within the plotted region as well. A low range of $z_{EC} < 1$ causes an overdamping of the well-sized drive and cannot prevent the underdamping of an undersized cylinder. Settings of $z_{EC} > 2$ results in the underdamping and can be suitable only for very oversized cylinder drives.

Therefore, a first improvement of the end cushioning design can be derived from the last point: the effective setting of the studied cushioning throttle corresponds to $1 < z_{EC} < 2$ rev. or to $2.2 < C_{EC} < 8$ Nl·(min·bar)$^{-1}$ in terms of pneumatic conductance. The accuracy of the setting can be increased, when this mostly relevant conductance range is spread over a wider range of throttle revolutions, as exemplary illustrated in **Figure 5**.

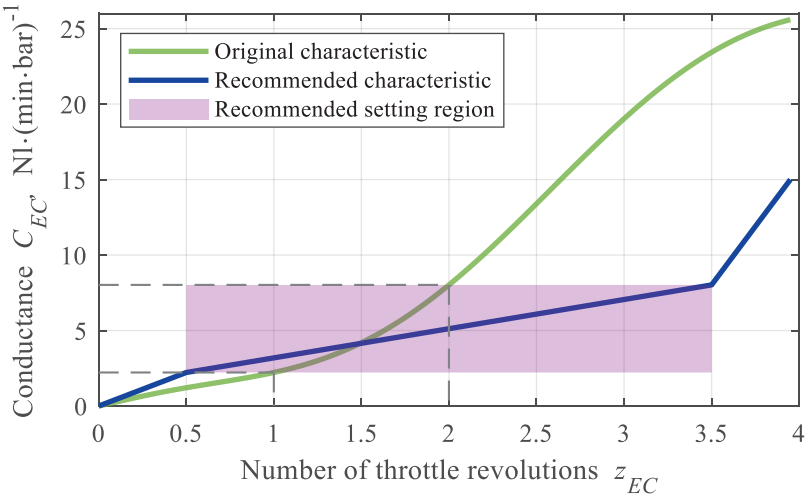


Figure 5: Conductance vs. opening characteristic of the cushion throttle, measured for the studied cylinder [12], and an example of improved characteristic with setting region spread over three knob revolutions instead of one.

The improved form of the conductance-opening characteristic covers the relevant range of C_{EC} within three throttle revolutions, smoothing the gradient dC_{EC}/dz_{EC}. This simple measure requires only a change of the throttle geometry and causes no extra costs since this profile must be designed only once. The outer dimensions of the throttle cartridge, installed in the cylinder head can be preserved. The result is an easier throttle setting for an end user. Hence this measure contributes to the aim 3, defined in the paragraph 1.2.

3 Sensitivity analysis

To increase the robustness of the end cushioning device against the changes in operational and environmental conditions by means of robust optimization, the design parameters with a major impact on the cushioning process must be found firstly. For this purpose, the sensitivity analysis (SA) is applied. The SA leads to an order reduction

of the optimization problem, due to only relevant parameters with a highest influence must be optimized, whereas the effect of the non-important factors can be neglected, and these parameters can be kept constant.

In the given case, impact of $n = 18$ parameters was studied by means of SA. These parameters can be divided into geometrical parameters ($x_1 \ldots x_4$), thermal model parameters ($x_5 \ldots x_9$) and parameters of the friction model ($x_{10} \ldots x_{18}$) according to [12]. Parameter x_9, the environmental temperature, which was assumed to be equal to the compressed air temperature in this study, is rather an operational parameter and not a design parameter. However, unlike the other operational parameters such as supply pressure, mass, or travel speed, whose high impact on the cushioning process is obvious, the influence of the air temperature is ambiguous and therefore was studied here.

The settings of z_{MO}, z_{EC}, m and p_0 were kept constant within the SA. The parametrisation was caried out for $\Omega = 1.5$, $z_{MO} = 15.15$ rev., and $z_{EC} = 1.75$ rev, due to a stable operation of the drive is feasible in the region adjacent to this point according to Figure 4. The preliminary analysis has also shown that the results of SA are similar at different supply pressures p_0, hence $p_0 = 7$ bar_{abs} was also kept constant within this step.

The sensitivity of two quality criteria **y**, i. e. model outputs F_{impact} and t_s, against the variation of parameters **x** was studied. Variation range of **x** was confined by reasonable from a technical point of view values of these parameters. Because of a wide variation range, expected additivity of the parameters influence, non-linearity, and non-monotonicity of the model, the local sensitivity analysis and one-at-a-time methods were considered as impropriate for this purpose [15]. Hence the sensitivity was studied with global methods based on the estimation of the Sobol's sensitivity indices and the Fourier Amplitude Sensitivity Test (FAST). The model was tested with nine SA-algorithms, based on these methods, which are implemented in the R Sensitivity Package [16]. Due to the results being very similar for all the methods, the evaluation only for the FAST is presented here in **Figure 6**.

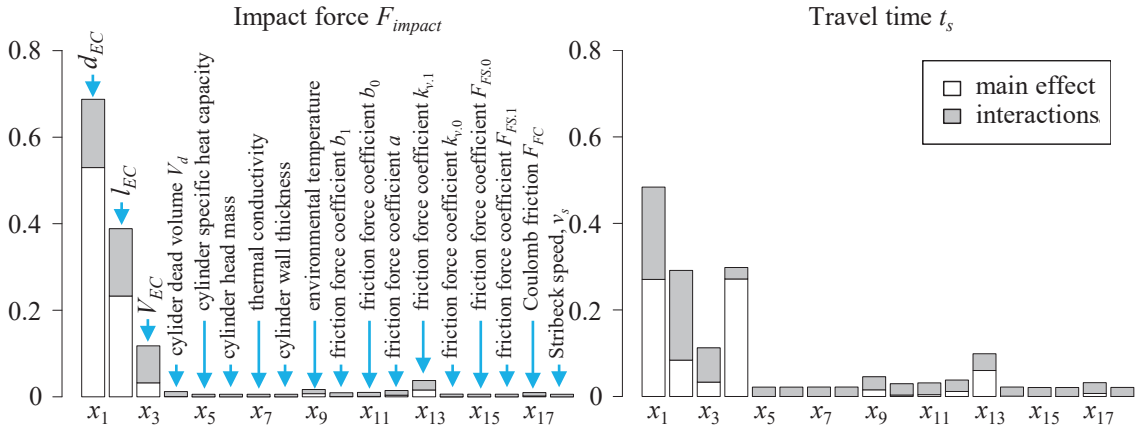


Figure 6: Results of the SA performed with FAST method, 4096 samples for model outputs F_{impact} and t_s.

To reach a reliable result at least 4096 samples were needed to keep the residuals of the sensitivity estimates under 3 %. From the results can be obtained that all four geometrical parameters $x_1 \ldots x_4$ have the highest impact on the cushioning quality in terms of both main effects (i. e. impact measure of a solely parameter varied) and interactions (i. e. measure of the system's sensitivity on simultaneous variation of many parameters). Besides the geometrical parameters, only environmental temperature T_0 (x_9) and speed- and pressure-proportional frictional coefficient $k_{v.1}$ (x_{13}) have a considerable influence. The other factors are less relevant and can be kept constant within optimization.

Due to this study focuses rather on simple implementable and low-cost measures of the damping quality improvement, the optimization of the factor x_{13} does not seem to be prospective, because there are no simple measures to adjust this factor to some desired value during the engineering process and to enable a persistence of this value during the operation of the cylinder's tribological system. The optimization of temperature T_0 is meaningless as well, however it should be treated as a noise factor because it: i.) impacts the damping quality, ii.) may naturally vary during the cylinder operation.

Furthermore, it needs to be mentioned that the tube length, which is included in the factor x_4 (dead volume of the cylinder drive), is subject to application and installation specifics and is not a constant parameter of the cylinder.

Therefore, only the first three factors, cushioning sleeve diameter d_{EC}, cushioning length l_{EC}, and cushioning dead volume v_{EC}, are qualified for the optimization.

4 Robust Optimization

Previously, three model outputs were considered as evaluation criteria of the damping quality: F_{impact}, $\ddot{x}_{max}$, and t_s. Unlikely deceleration $\ddot{x}_{max}$ and impact force F_{impact}, the stroke time t_s must not be necessarily minimized, because keeping it beneath the boundary $t_s < 0.3$ s is enough for the task. The deceleration is coupled with the impact force by mass m, hence only impact force F_{impact} can be used as an optimization function **y** to be minimized.

Four noise parameters **u** were set: inertial mass m, supply pressure p_0, setting of the meter-out throttle z_{MO} (to imitate the variance of the piston speed, e. g. due to a sealing wear after a long operation) and environmental temperature T_0. The robust optimization was performed for different variation ranges of these factors: $\Delta \in \{2, 4, 10\}$ % of the nominal value. In case of p_0, the nominal value relative to the atmospheric pressure was considered here, because in the industrial applications it is usually measured and controlled as a relative and not absolute pressure. Nominal value of the temperature T_0 was considered in the absolute scale. For the opening z_{MO} the variation was counted for a single turn of the throttle knob. All values are summarized in Annex B. The optimal designs were calculated for the same end cushioning throttle setting, as in the SA, and the operation pressure $p_0 = 7$ bar_{abs} due to it corresponds to the middle of the studied pressure interval and is a typical pressure level for industrial applications. The nominal value of the moving mass m corresponds to those at $\Omega = 1.5$.

The design parameters **x** to be optimized are derived from the SA in the previous chapter: cushioning sleeve diameter d_{EC}, cushioning length l_{EC}, and dead volume V_{EC}. Hence, the optimization function can be specified as:

$$\min_{\mathbf{x}\in\mathbb{R}^3,\ \mathbf{u}\in\mathbb{R}^4} \left\{ F_{impact}(\mathbf{x},\mathbf{u}) : \quad t_s \le 0.3, \qquad \mathbf{u}\cdot(1-\Delta) \le \mathbf{u} \le \mathbf{u}\cdot(1+\Delta) \right\} \tag{5}$$

The optimization was performed in Matlab, using the pattern search method with LHS (Latin Hypercube Sampling) and genetic initial search algorithms [17]. This strategy was chosen because of high the non-monotonicity and numerous local optima, shown in Figure 3. For each variation range Δ, an optimal design was sought with both initial search algorithms. The initial values were set to the point, previously estimated with a non-robust optimization. All in all, five optimal designs were calculated: two for the noise level $\Delta = \pm 2$ % (one estimated with genetic algorithm and one with LHS), two for $\Delta = \pm 4$ %, and one for $\Delta = \pm 10$ % (LHS only, no feasible solution found with genetic initial search).

The results are tabulated in Annex C. The comparison of these five designs with an original one is summarized in the **Figure 7**. The figure consists of three subplots for F_{imact} and three subplots for t_s, corresponding to the ±2, 4 and 10 % noise parameters variation for each of both evaluation criteria. Each of these sublots represents the fluctuations of F_{imact} or t_s for pneumatic cylinder moving a mass corresponding to $\Omega = 1.5$ within the desired travel time $t_s = 0.3$ s at supply pressure $p_0 \in \{4, 7, 10\}$ bar_{abs}, estimated for every design (O – original design and optimal designs D1…D5 in accordance with an Annex C). The fluctuation of evaluation criteria is illustrated with boxplots. Boxes correspond to the data between the 25th and 75th percentile and are crossed with a median value. Outliers that are more than 1.5 times the interquartile range away from the body of the box are marked with red "+". The data for every boxplot result from the $8^4 = 4096$ simulations, run with the four varied noise parameters, each quasi-randomly sampled eight times with LHS from the uncertainty region of ±Δ from the nominal value.

Figure 7 proves that the design of the cushioning unit, specifically the geometrical parameters: cushioning sleeve diameter d_{EC}, length l_{EC}, and dead volume v_{EC}, defines its robustness against the changes on operation environment. The median values of F_{impact} and t_s depend on design, fluctuation amplitude $2\cdot\Delta$, and nominal operation conditions in terms of supply pressure p_0. Naturally, the higher the noise amplitude, the higher the variances of both criteria (i. e. some sort of gradient of the damping quality deterioration with increasing noise amplitude) and their median values (that is the level of the expected cushioning quality). A small box size points at high robustness and a low median value indicates high damping quality. The nominal operating pressure must be considered as well. Whilst the optimal designs were calculated for $p_0 = 7$ bar_{abs}, the cushioning performance in terms of t_s increases with p_0

(more values are lying beneath 0.3 s at 10 bar_{abs} than at 4 bar_{abs}) and vice versa in terms of F_{impact}. This conflictive paradigm, established during the analysis of Figure 3 for the original design, remains unchanged also for the optimized versions of the end cushioning unit.

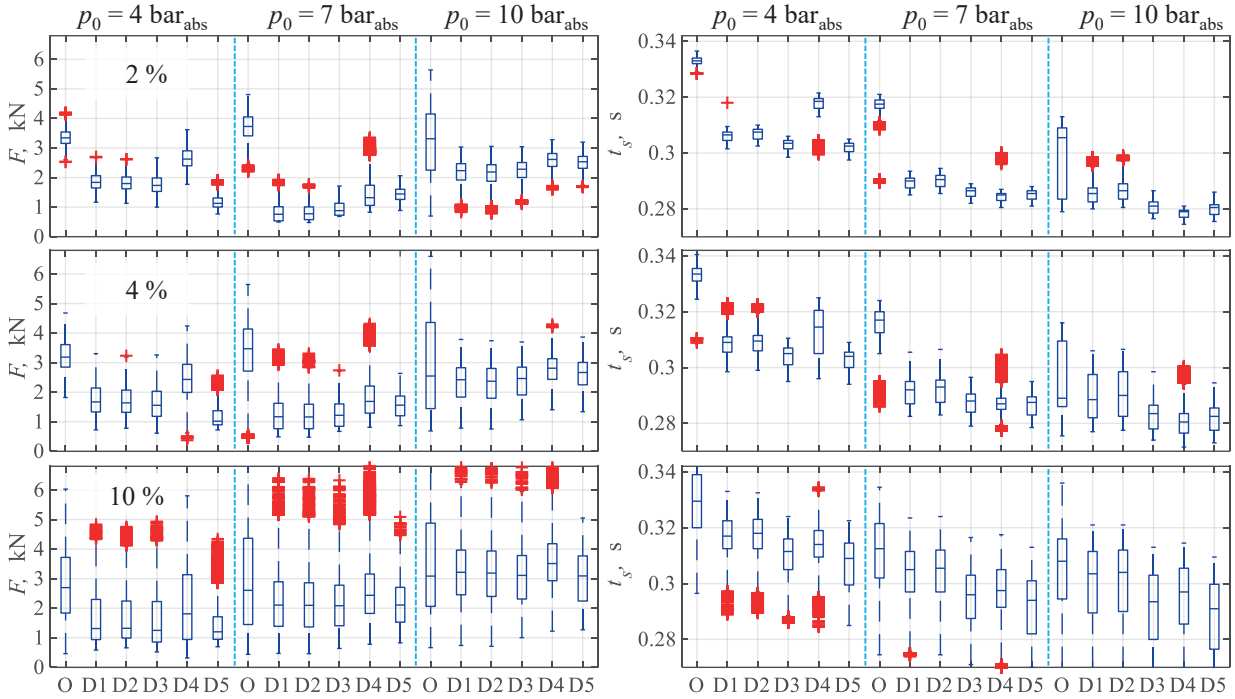


Figure 7: Evaluation of the robust optimization results plotted for two evaluation criteria F_{imact} (left) and t_s (right), three noise levels (±2 % for the top subplots, ±4 % for middle, and ±10 % for the bottom). Each boxplot assesses the variance of 4096 simulation results, estimated for 8 quasi-random samples of 4 noise parameters

The most important information, gained within this study is, however, that there are designs existing, that perform significantly better in all nine operation cases, plotted in the Figure 7, then the original design does. Especially interesting is that design D5, predicted to provide the best cushioning quality at high noise of ±10 % at p_0 = 7 bar_{abs}, provides the highest robustness (the smallest box size) in 7 of 9 cases for F_{impact}. It is slightly less robust then some of the other designs for t_s, but enables the highest damping quality (deepest median value) in 3 of 9 cases for F_{impact} and in 6 of 9 cases for t_s, and is competitive in the other cases as well. Generally, it can be said that this design is preferrable for a robust operation of a pneumatic cylinder under differently varying operating conditions and at various pressures, typical for pneumatic applications. On the other hand, there is no evidence that no other optimal designs are existing. Even though pattern search optimization method with both initial search algorithms performs good for functions with multiple optima, the result depends on the starting point and initial search algorithm itself.

5 Summary and Conclusion

The matter that the uncertainty in the operational conditions must be considered for a correct cylinder sizing is not new. The information presented within this paper offers a fundament for establishment of a method for systematic and intended calculation of the uncertainty influence on the cylinder sizing with regards to the damping capability of the pneumatic end cushioning by means of pneumatic frequency ratio PFR proposed by Doll et al. in [14]. In this paper is shown that PFR is handy for estimation of the cylinder's capability to dissipate the kinetic energy by the end of the stroke by means of standard integrated end cushioning. The damping capacity of a pneumatic cylinder is usually specified as the maximum kinetic energy that can be absorbed with the end cushioning. This value is easy to assess for highly oversized cylinders that travel at a nearly constant speed. In [14] is shown that a well-sized cylinder doesn't really reach a constant speed. That makes estimation of the kinetic energy hardly possible without sophisticated simulation tools or displacement transducer. This study proposes that for a well-

dimensioned cylinder a characterization of the damping capacity by means of PFR is more favorable, because the PFR can be easily calculated even when only cylinder size, pressure, desired travel time and mass are known.

For the exemplary analysed cylinder, operating at three pressures p_0 of 4, 7 and 10 bar_{abs} and travel times t_s of 0.25, 0.3 and 0.5 s an optimal value of PFR was assessed with $\Omega \approx 1.5$. It is shown that the user-friendliness of the end cushioning can be easily increased by changing the profile of the cushioning throttle characteristic, which simplifies the search for an optimal setting.

When a pneumatic cylinder is expected to operate at heavy conditions, such as:

- oscillating supply pressure, e. g. due to a pressure regulator hysteresis or pressure drop by synchronous extension of many drives,
- varying inertial load that may be the case in automating systems handling differently heavy objects,
- fluctuating travel speed caused by a meter-out throttle misalignment or changes in frictional behaviour,
- natural daily or seasonally environmental temperature changes, or compressed air temperature changes brought about by the compressor and air conditioning plant,

the cushioning performance can be increased by means of robust design optimization. In the given study the robust optimization was carried out after parameters with the highest impact on the damping quality, measured as travel time t_s and impact force F_{impact}, were identified within the sensitivity analysis. Three design parameters were chosen to be optimized: cushioning sleeve diameter d_{EC}, length l_{EC}, and dead volume V_{EC} to reach the minimal impact force F_{impact} within the travel time of $t_s < 0.3$ s under four operational and environmental parameters: inertial mass m, supply pressure p_0, setting of the meter-out throttle z_{MO}, and environmental temperature T_0, fluctuating in the vicinity of a nominal operation point within a range Δ.

By means of the robust optimization five designs were estimated and tested for 9 cases ($p_0 \in \{4, 7, 10\}$ bar_{abs} and $\Delta \in \{2, 4, 10\}$ %). The results show that all optimized designs perform better than the original one, and there is one design D5 existing that averages better than all the others.

The further work will be focused on the search of a globally optimal design or on bringing the evidence that the design D5 is already globally optimal. The next step is an experimental proof of robustness. For this purpose, a cylinder head will be manufactured with geometrical parameters corresponding to the globally optimal design and the end cushioning throttle with characteristic close to the shown on Figure 5. Furthermore, the proposed methodology will be validated on a larger cylinder to prove its transferability on the other cylinder designs.

Summing up, the measures proposed in this paper and to be continued and refined within the following steps, can provide a versatile, low-cost improvement of standard pneumatic end cushioning. This increases the attractiveness of pneumatic applications due to an easier use, higher energy efficiency in terms of oversizing prevention of cylinders, applied for the motion-tasks, and enabling a robust cushioning effect even in challenging, fluctuating conditions.

6 Founding Sources

This research is funded by the European Social Fund and co-financed by tax funds based on the budget approved by the members of the Saxon State Parliament.

Diese Maßnahme wird mit Mitteln aus dem Europäischen Sozialfonds gefördert und mitfinanziert durch Steuermittel auf Grundlage des von den Abgeordneten des Sächsischen Landtags beschlossenen Haushaltes.

7 Annex

Annex A. Values of inertial load m corresponding to the PFRs Ω and supply pressures p_0 for the Figure 3.

Ω	p_0 = 4 bar_{abs}	p_0 = 7 bar_{abs}	p_0 = 10 bar_{abs}
1.4	11.8 kg	20.7 kg	29.6 kg
1.5	10.3 kg	18.1 kg	25.8 kg
1.6	9.1 kg	15.9 kg	22.7 kg
1.8	7.2 kg	12.5 kg	17.9 kg
2.0	5.8 kg	10.2 kg	14.5 kg

Annex B. Variation of the noise factors for the robust optimization: p_0 –supply pressure, m – inertial load, z_{MO} – meter-out throttle opening, T_0 – environmental and compressed air temperature.

No. of case	*Noise* Δ, %	*Nominal* p_0, bar_{abs}	Variation ranges			
			p_0, bar_{rel}	*m*, kg	z_{MO}, °rev.	T_0, K
1	±2	4	±0.06	±0.206	±7.2°	±5.86
2		7	±0.12	±0.362		
3		10	±0.18	±0.516		
4	±4	4	±0.12	±0.412	±14.4°	±11.7
5		7	±0.24	±0.724		
6		10	±0.36	±1.032		
7	±10	4	±0.3	±1	±36°	±29.3
8		7	±0.6	±1.81		
9		10	±0.9	±2.58		

Annex C. Designs of the integrated pneumatic end cushioning: original design (O) and optimized designs D1...5.

Design	Estimated for:	Initial search algorithm	d_{EC}, m	l_{EC}, m	V_{EC}, cm^3
O	-	-	0.016	0.016	1.62
D1	p_0 = 7 bar_{abs}, Δ = ±2%	genetic	0.0172	0.0168	0.88
D2	p_0 = 7 bar_{abs}, Δ = ±2%	LHS	0.0174	0.0174	0.91
D3	p_0 = 7 bar_{abs}, Δ = ±4%	genetic	0.0169	0.0136	0.42
D4	p_0 = 7 bar_{abs}, Δ = ±4%	LHS	0.0142	0.0109	0.56
D5	p_0 = 7 bar_{abs}, Δ = ±10%	LHS	0.017	0.0125	0.18

Nomenclature

Variable	*Description*	*Unit*
A	Surface area	[m²]
c	Spring stiffness	[N·m^{-1}]
C	Pneumatic conductance	[Nl·(min·bar)$^{-1}$]
F	Force	[N]
h	Thickness of elastomer shock absorber	[m]
i	Number of evaluation criteria (model outputs)	[-]
k	Number of noise parameters	[-]
l	Length	[m]
m	Inertial mass	[kg]
n	Number of design parameters	[-]
p	Pressure	[bar]
t	time	[s]
T	Temperature	[K]
$\mathbf{u}$	Vector of noise parameters	[-]
V	Volume	[m^3]
x	Piston coordinate	[m]
$\dot{x}$	Piston speed	[m·s^{-1}]
$\ddot{x}$	Piston acceleration	[m·s^{-2}]
$\mathbf{x}$	Vector of design parameters	[-]
$\mathbf{y}$	Vector of evaluation criteria (model outputs)	[-]
z	Number of throttle knob revolutions	[rev.]
Δ	Variation of the noise parameters	[-]
ν	Polytropic exponent	[-]
ω	Frequency	[Hz]
Ω	Pneumatic frequency ratio (PFR)	[-]

Index

Description	*Relation to*
0	Supply air conditions
a	Ambient, atmospheric
abs	Absolute (pressure)
A	Cylinder chamber A

B	Cylinder chamber B
EC	End cushioning
d	Dead (volume)
rel	Relative (pressure)
s	Setting
thr	Threshold value

References

[1] Report: *EnEffAH: Energy efficiency in production in the drive and handling technology field: Basic principles and measures*, EnEffAH Project Consortium, Stuttgart, 2012. Last access on October 25, 2021: https://www.eneffah.de/EnEffAH_Broschuere_engl.pdf.

[2] White Paper: ITT Enidine Inc. *Shock Absorbers and Rate Controls*.

[3] White paper: ACE NoCushion Serie. *Externe Endlagendämpfung für Pneumatikzylinder*.

[4] White paper: AIRTECs InnoMotix®-System. *Pneumatik ohne Dämpfer*.

[5] White paper: Festo SE & Co. KG. *Motion Terminal VTEM*.

[6] White paper: Aventics GmbH. *Pneumatische Endlagendämpfung. Zylinder optimal einstellen: CAT – Cushioning Adjustment Tool*.

[7] Festo AG & Co. Patent DE19637291C2: *Vorrichtung zur Endlagendämpfung*, 13.12.2001.

[8] Wang, Y. T. et al., *Computer Simulation of a Shock-Absorbing Pneumatic Cylinder*, In: Journal of Sound and Vibration, Vol. 93(3), pp. 353-364, 1984.

[9] Beater, P., *Endlagendämpfung pneumatischer Zylinder*, In: O+P Ölhydraulik und Pneumatik, Vol. 47 (2003), No. 3, pp 163-167, 2003.

[10] Dvořák, L. et al., *Experimental Verification of Pneumatic Cylinder External Pneumatic Cushioning*, EPJ Web of Conferences, Vol. 213, EFM18 – Experimental Fluid Mechanics, pp. 1-4, 2018, DOI: https://doi.org/10.1051/epjconf/201921302015

[11] Gerc, E.V., Krejninm G.V., *Rasčet pnevmoprivodov: spravočnoe posobie*, Mashinostoenie, Moscow, USSR, 1975.

[12] Nazarov, F., Weber, J., *Modelling, Simulation and Validation of the Pneumatic End-Position Cylinder Cushioning*, The 17th SICFP'21, May 31 – June 2, 2021, Linköping, Sweden, pp. 206-223, 2021.

[13] Nazarov, F., Weber, J., *Heat Transfer Model of Pneumatic End-Position Cylinder Cushioning*, International Journal of Fluid Power, Vol. 23, SICFP 2021 Issue 1, pp. 1-18, DOI: https://doi.org/10.13052/ijfp1439-9776.2311

[14] Doll, M., Neumann, R., Sawodny, O., *Dimensioning of Pneumatic Cylinder for Motion Tasks*, International Journal of Fluid Power, Vol. 16, No. 1, pp. 11-24, DOI: https://doi.org/10.1080/14399776.2015.1012437

[15] Saltelli, A., Chan, K., Scott, E. M., *Sensitivity analysis*, The Wiley Paperback Series, 2009.

[16] Iooss, B. et al, *Global Sensitivity Analysis of Model Outputs: Documentation to R Package 'sensitivity'*, October 20, 2021.

[17] The MathWorks Inc., *Pattern Search Options*, https://de.mathworks.com/help/gads/pattern-search-options.html, visited on January 8, 2022.